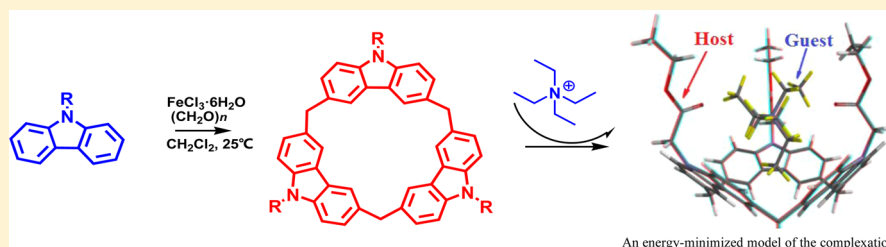


Calix[3]carbazole: One-Step Synthesis and Host–Guest Binding

Peng Yang,* Yong Jian,[†] Xue Zhou,[†] Gang Li, Tuo Deng, Hongyan Shen, Zhaozheng Yang, and Zhangmin Tian

Key Laboratory of Structure-Based Drug Design and Discovery of Ministry of Education, Shenyang Pharmaceutical University, Shenyang 110016, People's Republic of China

Supporting Information



ABSTRACT: The one-step synthetic strategy for the preparation of the hitherto unknown calix[3]carbazole from readily available starting materials is described. Calix[3]carbazole is obtained in 20% yield, and it could selectively bind the $N(C_2H_5)_4^+$ cation (tetraethylammonium, TEA) via cation– π interactions. The experimental and modeling results indicate that calix[3]carbazole possesses a larger π -cavity as well as a better chromophoric property than the traditional phenol-based macrocycles, and thus is capable of binding to and optically responding to the relatively large guest TEA.

INTRODUCTION

It is always a fascinating job of chemists to construct novel macrocyclic architectures capable of achieving the activities of enzymes.¹ In nature, proteins often use the π -electrons of the aromatic side chains (benzene, phenol, and indole) of Phe, Tyr, and Trp to accommodate various cations.² A well-known example is the method of acetylcholine binding to its receptor acetylcholinesterase (AChE), in which the quaternary ammonium moiety of the choline ion is bound chiefly by the aromatic box of AChE.^{2a} In view of this unique property of proteins, a considerable amount of macrocycles, e.g., cyclophanes, calixarenes, resorcinarenes, cyclotrimeratrylenes (CTVs), pillararenes, calixpyrroles, calixindoles, and calixnaphthalenes, have been developed, and their cation– π binding properties have been extensively investigated as well.^{2b}

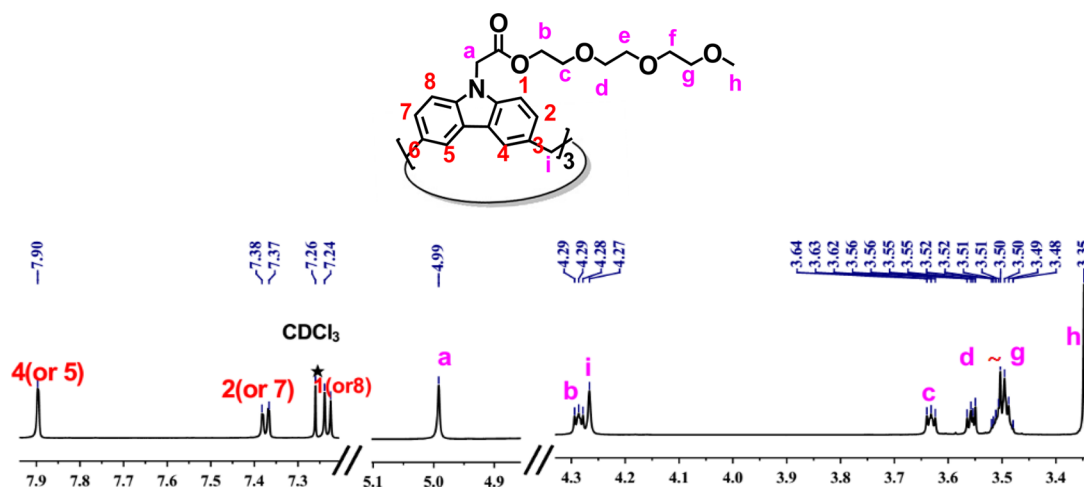
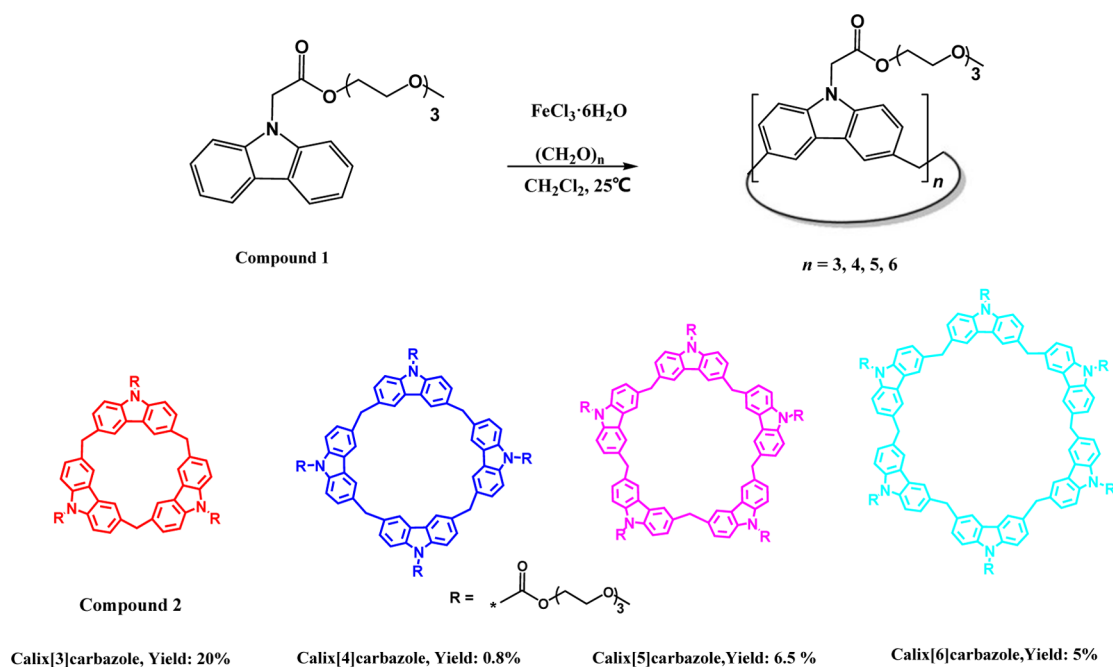
The traditional phenol-based macrocycles, such as calix[4]-arene, resorcinarene, and CTV, generally possess small cavities so that they could only accommodate small cationic guests, such as NH_4^+ and/or $N(CH_3)_4^+$ cations. However, the macrocycles possessing a relatively large cavity would have more interesting applications, e.g., nanoscale reaction vessels.^{4a–c} A general way of expanding the cavities of these phenol-based macrocycles is to construct cavitands or cage compounds. These structurally modified molecules would have enough space to accommodate the relatively large guests (e.g., tetraethylammonium, TEA^{4d}) as well as to catalyze the reactions.^{4a,b} However, their preparations usually require multistep synthesis/purification and sometimes are difficult.^{4c} The development of structurally novel, large hosts in an easier way continues to be an attractive job of chemists in the field of calixarene chemistry.

In nature, indole is the strongest π -donor among the three aromatic side chains of Phe, Tyr, and Trp that proteins utilize to interact with cations.² Generally speaking, a compound with a more extended π -surface possesses a higher π -donating ability as well as a better chromophoric property. Taken together, we envision that a novel calixarene, using a π -extended analogue of indole as the basic skeleton, would possess a larger π -cavity, a higher π -donating ability, and a better chromophoric property than the traditional phenol-based macrocycles. As such, by one-step construction of such an expanded macrocycle to accommodate a large guest, not only can the synthetic work be simplified, but also the convenient and inexpensive UV–vis and fluorescence techniques can be used to monitor the host–guest binding behaviors. Following our long-term interests in DNA binders,⁵ we recently synthesized a novel biscarbazole-based DNA ligand.^{5a} The unexpected synthesis of the methylene-bridged biscarbazole in that work inspired us to construct a carbazolyl calixarene. Indeed, carbazole, the π -extended indole, has been extensively investigated in the studies of optical-electrical materials,⁶ optical signaling reporters,⁷ and protein kinase inhibitors.⁸ Carbazoles have also been used as the building blocks to construct novel calixarenes. For some examples, Jonathan L. Sessler's group reported that a carbazole-expanded calixpyrrole could bind an anion guest and could optically report the recognition of the guest.^{9a} Very recently, a carbazolyl cyclophane was synthesized in a yield of 3%.^{9b} This interesting molecule does possess a cup-shaped cavity and may have potential guest-binding properties to explore. However,

Received: February 3, 2016

Published: March 11, 2016

Scheme 1. Synthesis of Calix[3]carbazole

Figure 1. Partial ^1H NMR (600 MHz) spectrum of calix[3]carbazole in CDCl_3 at 25°C .

multistep syntheses are often required to prepare these carbazolyl cyclophanes, and the yields are usually not satisfying. These deficiencies would obstruct their further structural modifications and functional explorations. Herein, we report a facile one-step synthesis of calix[3]carbazole as well as its binding properties to alkylammonium cations.

RESULTS AND DISCUSSION

The synthesis of **1** (Scheme 1), the starting material, was straightforward. The side chain of methoxytriglycol acetate was selected both for its good solubility in various solvents (e.g., CH_2Cl_2 , CHCl_3 , MeCN, a mixture of MeCN and H_2O) and for the further functionalization of the ester group in the future. This Friedel–Crafts alkylation of **1** was initially conducted using conditions similar to those for the preparation of linear carbazolyl oligomers/polymers,¹⁰ but all trials were unsuccessful. We then used CH_2Cl_2 to run this reaction. Various catalysts were examined: using H_2SO_4 and AlCl_3 , only polymers were produced, TsOH and $\text{BF}_3 \cdot \text{O}(\text{C}_2\text{H}_5)_2$ could generate the desired

cyclic product, but the yields were unreproducible, and both FeCl_3 and $\text{FeCl}_3 \cdot 6\text{H}_2\text{O}$ gave reliable yields. The optimized reaction time was 8–10 h, and extending the time only favored the formation of polymers. The major product of calix[3]carbazole (**2**; yield 20%) could be successfully isolated by regular silica column chromatography, and no linear[3]carbazole was detected. It has been fully characterized (Figures S4–S6 and S23–S26). Moreover, the byproducts of calix[4]carbazole (yield 0.8%), calix[5]carbazole (yield 6.5%), and calix[6]carbazole (yield 5%) have also been found (Figures S7–S15). However, these byproducts usually contained traces of linear oligomers, which made their purifications difficult. Nevertheless, the target compound of calix[3]carbazole could be readily obtained, and it is of interest to explore its potential properties.

The bridging methylene of the calix[4]arene (and/or CTV) in a “cone” conformation usually displays the resonance signal of a pair of doublets.³ However, the bridging methylene of **2** showed a singlet resonance at ~ 4.27 ppm in its ^1H NMR

spectrum (Figure 1 and Figure S4). Moreover, this singlet peak was not split even at $-80\text{ }^{\circ}\text{C}$, and it became broad at $-92\text{ }^{\circ}\text{C}$ (Figure S16a). It indicated that **2** possessed either (i) a rapidly inverted cone conformation on the NMR time scale or (ii) a distorted or flattened partial cone conformation (e.g., the saddle conformation of CTV^{3e}). In spite of the conformational mobility, the former conformation is more interesting than the latter one because a macrocycle in a cone conformation may have the capacity to serve as the “container” for guest molecules.³ X-ray crystallographic data are useful for learning the geometry of this cyclic trimer in the solid phase. Unfortunately, our numerous efforts to obtain a suitable single crystal were fruitless. We then resorted to the host–guest binding experiments and examined the binding abilities of **2** to the cationic guests in Figure 2. As the basic cation– π binding

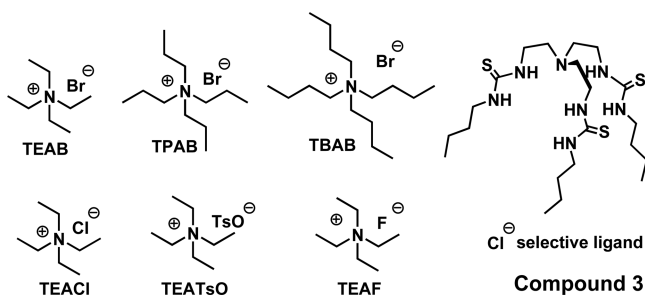


Figure 2. Tested guests and the chloride anion ligand **3**.

experiments performed in low-polarity/lipophilic solvents could help in learning the geometry and the size of a potential π -cavity of a neutral host,^{2b,11} all our experiments were performed in either CHCl_3 or CH_2Cl_2 .

The UV–vis and fluorescence spectra of both **1** and **2** were first examined (Figures S18 and S19). It could be seen that the spectral patterns of **2** were similar to those of **1** (the control compound, similarly hereinafter). As such, the absorption peaks at ~ 300 and ~ 351 nm in Figure S18b should be assigned to the $^1L_a \leftarrow ^1A$ and $^1L_b \leftarrow ^1A$ transitions of the carbazole moiety of **2**, respectively.^{5a,12} The peaks at ~ 358 and ~ 375 nm in Figure S19b should be ascribed to the emission of the carbazole moiety as well. Owing to the decent chromophoric properties of **2**, both UV–vis and fluorescence spectra were used to detect its guest-binding abilities. As shown in Figure 3, upon binding

to TEAB, both the weakening of the absorption peak of **2** at ~ 351 nm (hypochromic effect) and its gradually quenched emission were observed. Moreover, a clearly observed isosbestic point at ~ 355 nm (Figure 3a) illustrated that there existed only one predominant complexation in the current host–guest binding system. It is generally accepted that the existence of the isosbestic point in the spectra of UV–vis titration indicates the binding process is a specific interaction. As a control, TEAB neither weakened the peak of the $^1L_b \leftarrow ^1A$ transition of **1** nor quenched its fluorescence (Figure S20). Moreover, both TPAB and TBAB could not weaken the absorption peak of **2** (Figure S21a,b) or quench its fluorescence (Figure S22a,b), which indicated that they did not bind to **2**. The above spectral behaviors indicated that **2** might possess a well-defined cavity so that its rich π -electrons could interact with TEA rather than TPA and TBA cations. Because the properties of carbazoles upon binding to cationic guests have rarely been reported, we could not find the spectral features caused by their π -cation interactions for comparison. As such, we resorted to comparing the above spectral patterns with those displayed by indole's derivatives, the cousins of carbazoles. Fortunately, an analogous hypochromic effect caused by the cation– π interaction between the K^+ ion and an indolyl compound (IE18C6, a crown ether linked by double indoles^{13a}) has been reported.^{13b} The resemblance of the optical signaling patterns between the above case and our findings indicated that the binding of **2** to TEA should take place via cation– π interactions.

The above behavior could qualitatively illustrate the **2**–TEA binding nature. However, the insignificant changes of the signals of both UV–vis and fluorescence spectra may cause errors for the accurate determination of K_a . We then performed ^1H NMR to further study the properties of **2** upon binding to TEA. To preclude the possibility of the intermolecular interactions of **2** itself, the ^1H NMR spectra of **2** at various concentrations were first examined (Figure S17). It could be seen that **2** did not aggregate even at a concentration of 30 mM. All the ^1H NMR titrations were then conducted at a 5 mM concentration of **2**. Figure 4 lists the partial ^1H NMR spectra of **2** upon binding to TEA(TsO) (TEA with the counteranion *p*-toluenesulfonate). The full titration spectra are presented in Figure S29. It could be seen that the mutual interactions made protons *n* and *m* of TEA shift upfield ($\Delta\delta = 0.34$ and 0.26 ppm, respectively). Meanwhile, proton 4 (or 5)

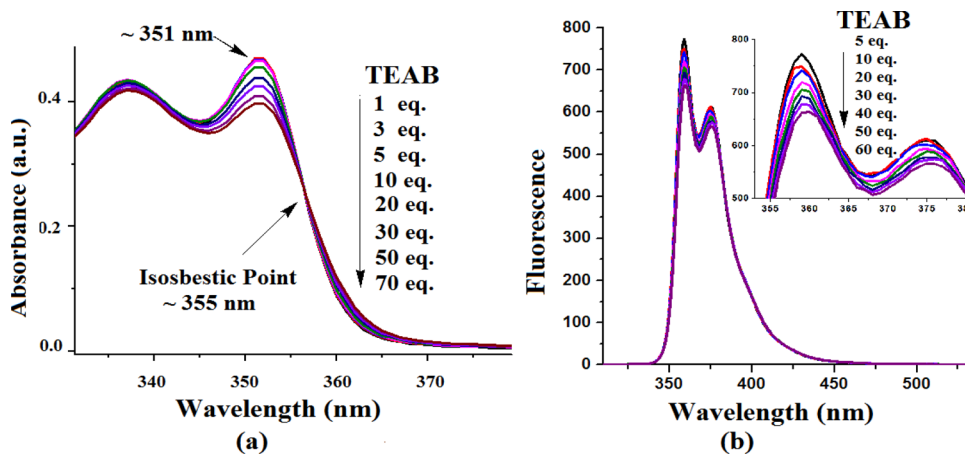


Figure 3. Upon addition of TEAB at $25\text{ }^{\circ}\text{C}$: (a) UV–vis spectra of **2** (50 μM) in CHCl_3 ; (b) fluorescence spectra of **2** (30 μM) in CH_2Cl_2 (excitation wavelength 302 nm).

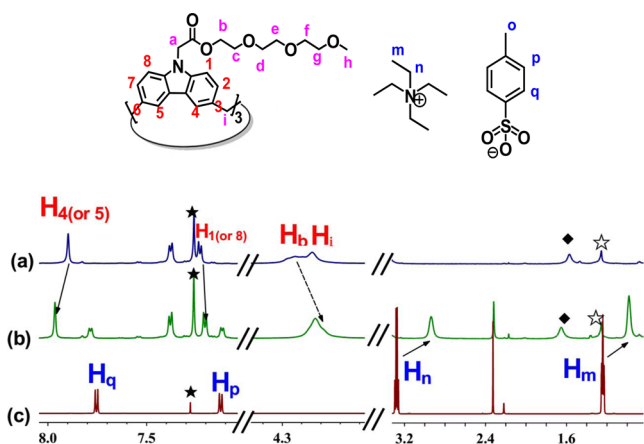


Figure 4. Partial ^1H NMR (600 MHz, 25 $^\circ\text{C}$, CDCl_3) spectra of (a) **2** (5 mM), (b) **2** (5 mM) + TEA(TsO) (8 mM), and (c) TEA(TsO) (8 mM) (\star , CDCl_3 ; \blacklozenge , H_2O ; \star , impurity).

of **2** showed a downfield shift ($\Delta\delta = 0.06$ ppm), and its proton 1 (or 8) showed an upfield shift ($\Delta\delta = 0.03$ ppm). The fact that only the average signals of the complexed and the free guests were observed in the spectra indicates that the formation and dissociation of the current host–guest complex were too fast on the NMR time scale. The above behavior clearly illustrated that the TEA cation interacted with the π -electrons of the carbazole aromatic system. Moreover, the upfield shift ($\Delta\delta = 0.03$ ppm) of proton b was also observed, indicating the interaction between the ester groups of **2** and TEA. According to Stefano Roelens and his co-workers' findings,¹¹ the binding of the ester groups to the ammonium ion was probably driven by the first generated cation– π interactions. In other words, their bindings took place cooperatively. As a control, in the ^1H NMR spectra of **1** upon binding to TEA(TsO) (Figure S36), neither the protons of the host nor the protons of the guest showed chemical shift changes.

VT NMR spectra of an equimolar mixture of **2**–TEA(TsO) were recorded (Figure 5 and Figure S16b). It could be seen from Figure 5 that when the temperature decreased, both Hn and Hm of TEA became broad and shifted gradually upfield. This indicated the binding affinity of **2** to TEA increased with a decrease of the temperature. It could also be observed from Figure 5 that the singlet signal of the bridging methylene of **2**

became broad gradually with a decrease of the temperature and split into two peaks at -80 $^\circ\text{C}$. This behavior clearly demonstrated that the fast exchanged formation and dissociation of **2**–TEA complexation had been slowed down at low temperature. As such, the splitting signals of the bridging methylene of **2** were observed due to the constrained C_{3v} conformation (or cone conformation) of **2**.

2D NOESY spectra of the **2**–TEA complexation were recorded at 25 and -92 $^\circ\text{C}$, respectively (Figure 6 and Figure S27). At both temperatures, the cross-peak between proton m (Hm) of TEA and proton 4 (or 5) (H4 (or H5)) of the carbazole moiety of **2** was observed. At 25 $^\circ\text{C}$, the pattern of the cross-peak appeared to be a “contour”, whereas the circles of their cross-peak at -92 $^\circ\text{C}$ became more “solid” due to the increased binding strength of **2**–TEA complexation at the lower temperature. Moreover, at 25 $^\circ\text{C}$, the intermolecular cross-peak between H4 (or H5) of **2** and Hm of TEA was found to be in the opposite phase compared with the intramolecular cross-peaks of the host itself. At -92 $^\circ\text{C}$, however, this intermolecular cross-peak was in the same phase as the intramolecular cross-peaks of the host. According to ref 14, the above behaviors were possibly caused by the differences between the intramolecular and the intermolecular correlation times at different temperatures. In other words, at 25 $^\circ\text{C}$, the cation– π binding affinity of **2**–TEA complexation is relatively weak, so that the correlation time for **2**–TEA complexation is different from that for **2** at 25 $^\circ\text{C}$ due to the different tumbling dynamics of the intermolecular/intramolecular NOE correlations. At -92 $^\circ\text{C}$, however, the **2**–TEA binding affinity becomes strong, so that the complexation may tumble at a rate similar to that of the host, and thus resulting in their closer correlation times.

A simple energy-minimized model of **2**–TEA complexation (Figure 7) indicated that one ethyl tail of TEA resided in the deep cavity of **2** while three carbonyl moieties of the ester groups of **2** were oriented to TEA.¹⁵ The modeling result was consistent with the findings from ^1H NMR studies. It should be pointed out that the protons of the *p*-toluenesulfonate moiety of TEA(TsO) showed neither a chemical shift nor cross-peaks with the protons of **2**.

Both the Job plot (Figure S28a) and HRMS spectrum (Figure S28b), in which an equimolar mixture of the $[\mathbf{2} + \text{TEA}]^+$ (m/z) complex was found to be the major peak, revealed that the binding stoichiometry of **2**–TEA was 1:1.

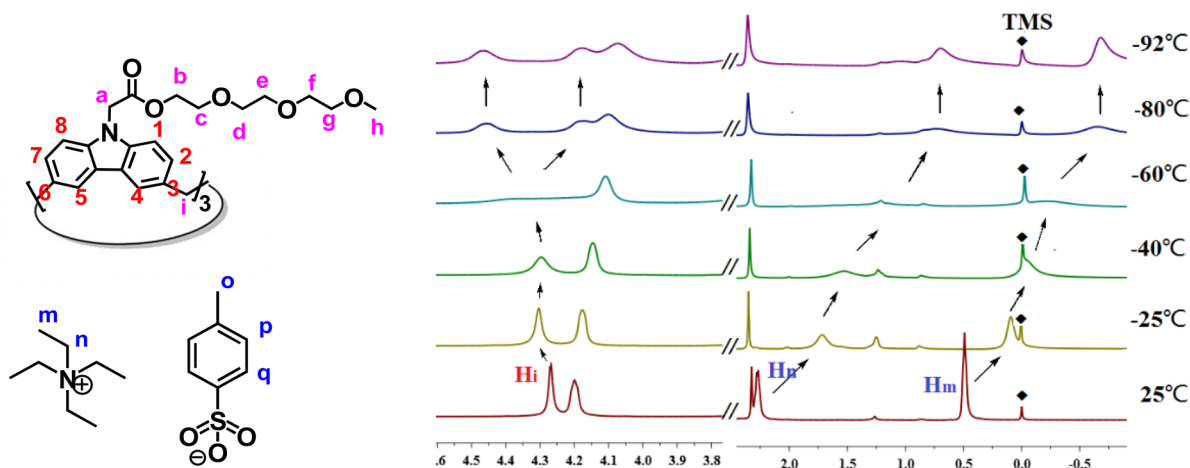


Figure 5. VT NMR spectra of an equimolar mixture of **2** + TEA in CD_2Cl_2 (25, -25 , -40 , -60 , -80 , and -92 $^\circ\text{C}$).

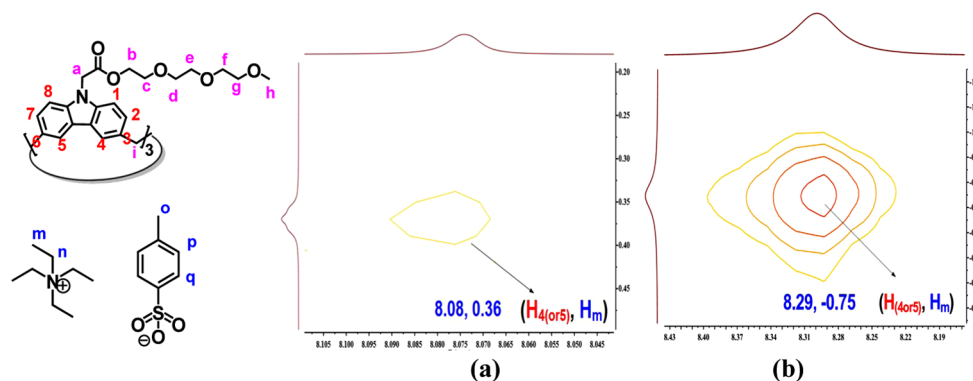


Figure 6. Partial 2D NOESY spectrum of an equimolar mixture of **2** + TEA: (a) at 25 °C; (b) at -92 °C.

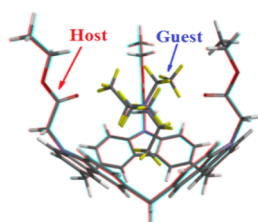


Figure 7. Energy-minimized model of the complexation.¹⁵ Host: C = dark gray, H = light gray, N = blue, O = red. Guest: C = dark gray, H = yellow.

Such a result also confirmed the assumption proposed from the analysis of UV-vis titration: solely one host-guest complexation existed. Moreover, the nonlinear least-squares fitting of the chemical shifts of H4 (or H5) in Figure S29 to a 1:1 stoichiometric model^{3d,16} gave a satisfactory R^2 value (0.98, Figure S37d and Table 1). The calculated association constant

Table 1. Association Constants of **2** Binding with Various Guests in CDCl_3 ^a

	K_a (E) (M^{-1})	$-\Delta G$ (kJ/mol)	R^2
TEAB	50.5 (2.4)	9.7	0.99
TEA(Cl)	66.3 (3.5)	10.4	0.99
TEA(Cl)/dual hosts	353.4 (36.5)	14.5	0.98
TEAF	66.8 (4.1)	10.4	0.99
TEA(TsO)	26.8 (1.6)	8.1	0.98
TPAB	–	–	–
TBAB	–	–	–

^aE is the standard error of the nonlinear least-squares fitting of the titration curves in Figure S37. The symbol “–” indicates no binding. $-\Delta G$ was calculated on the basis of the Van't Hoff isotherm equation $\Delta G = -RT \ln K$. These data were calculated by fitting the changes of the chemical shift of H4 (or H5).

K_a for **2**-TEA(TsO) complexation was about 26.8 M^{-1} . The binding affinities between **2** and the other selected guests (Figure 2) were also examined (Figures S30–S34 and S37 and Table 1). Consistent with the preliminary results from both UV-vis and fluorescence titrations, **2** did not bind TPAB and TBAB. Counteranions slightly affected the binding affinities of **2** to the TEA cation, and the ranking was $\text{TEA(Cl)} \approx \text{TEA(F)} > \text{TEA(B)} > \text{TEA(TsO)}$. The nonlinear least-squares fitting of the chemical shifts of H1 (or H8) of **2** in these ^1H NMR titration spectra gave the same ranking of their binding affinities (Figure S38 and Table S1).

Although it is generally accepted that the driving force endowed by π -electrons does not afford sufficient energy to separate the cation from the counteranion in apolar media, the anion-induced allosteric effect^{3g,17} can make that occur. A so-called “dual host strategy” would help to learn the counteranion's role played in the binding process of a host to a cationic guest.^{17a} Thus, the ^1H NMR spectra of **2** upon binding to TEA(Cl) in the presence of **3**¹⁸ (Figure 2), a known specific ligand of the chloride anion, were then recorded (Figure S35). As shown in Table 1, the association constant of **2** binding to TEA(Cl) was increased from 66.3 to 353.4 M^{-1} due to the weakening interaction of the ion pairs. This thus further validated that the cation- π interaction was the primary binding force for the **2**-TEA complexation.

CONCLUSIONS

In conclusion, inspired by the naturally occurring strong π -donor (indole, the side chain of Trp), we used carbazole, the π -extended indole, to construct a non-phenol-based macrocycle. Calix[3]carbazole was facily obtained via a one-step synthesis, and it could bind TEA primarily via π -cation interactions, which were validated by the studies of UV-vis, fluorescence, ^1H NMR and HRMS spectra.

Among the extensively reported macrocycles, CTVs may geometrically resemble calix[3]carbazole in view of their C_3 -symmetrical structures. However, calix[3]carbazole possesses a larger π -cavity and a better chromophoric property than CTVs so that it could interact with and optically respond to TEA, a guest larger than both NH_4^+ and $\text{N}(\text{CH}_3)_4^+$ cations. So far, the yield of calix[3]carbazole is not immensely satisfying. Challenging work remains to be done for further exploration of this just born “infant” of the macrocycle family, but considering its readily available starting materials, its facile one-step synthetic strategy, its large π -cavity, and its decent chromophoric property, we believe that our results will enrich the macrocycle chemistry. Also, considering the very broad applications of the parallel important carbazole chemistry, our findings may also shed light on the assessment of the hitherto unexplored optical-electronic as well as biological properties of this novel end-capped macrocycle.

EXPERIMENTAL SECTION

Experimental Protocol. Unless otherwise noted, the materials were obtained from commercial suppliers and were used without further purification. Thin-layer chromatography (TLC) analysis of the reaction mixtures was performed on F-254 TLC plates. Column chromatography was performed on 200–300 mesh silica gel. Fluorescence emission spectra were obtained at 298 K, and the

excitation wavelength was 302 nm with slit widths of 3 nm (excitation) and 1.5 nm (emission). UV-vis absorption spectra were obtained at 298 K. NMR spectra were recorded on a 600 MHz instrument for ^1H and a 150 MHz instrument for ^{13}C , unless otherwise specified. Chemical shifts are reported in parts per million, and all coupling constants (J values) are reported in hertz using TMS as the internal standard. High-resolution mass spectrometry (electrospray ionization, ESI) was carried out using a QTOF-MS instrument with an ESI source.

For all the measurements, the solutions of both **1** and **2** were freshly prepared before use. For UV-vis and ^1H NMR titrations, the stock solutions of various guests were prepared by dissolving them in CHCl_3 (1.0×10^{-1} M) and in CDCl_3 (5.0×10^{-1} M), respectively. Fluorescence titrations were performed in CH_2Cl_2 , and stock solutions of the guests were prepared in DMSO (3.0×10^{-1} M). Before the spectra were recorded, the sample solutions were mixed for 2 min after each addition of guests. Both UV-vis and fluorescence measurements were performed in a 1 cm cuvette. All the experiments were repeated three times at least.

Synthesis of Compound 1. The intermediate carbazole-9-acetic acid was synthesized following ref 19. Then 9.0 g of carbazole-9-acetic acid (0.04 mol), 19.7 g of triethylene glycol monomethyl ether, and 0.22 mL of H_2SO_4 (~ 0.004 mol) were dissolved in 80 mL of MeCN and refluxed for 15 h. After evaporation of the solvents under vacuum, the reactants were poured into 100 mL of ice-water, extracted with 3×100 mL of CH_2Cl_2 , and dried over anhydrous Na_2SO_4 . After removal of the solvents under reduced pressure, the residue was purified by flash chromatography on silica gel using MeOH/ CH_2Cl_2 (1:50, v/v) as the eluent to give the oily product. Yield: 10.5 g, 70.7%. ^1H NMR (600 MHz, CDCl_3): δ 8.09 (d, $J = 7.7$ Hz, 2H), 7.46 (t, $J = 8.2$ Hz, 2H), 7.35 (d, $J = 8.2$ Hz, 2H), 7.31–7.12 (m, 2H), 5.05 (s, 2H), 4.43–4.20 (m, 2H), 3.65–3.61 (m, 2H), 3.59 (dd, $J = 5.7, 3.7$ Hz, 2H), 3.54–3.51 (m, 4H), 3.48 (dd, $J = 6.1, 3.4$ Hz, 2H), 3.37 (s, 3H). ^{13}C NMR (150 MHz, CDCl_3): δ 168.4, 140.5, 125.9, 127.2, 123.2, 120.4, 119.6, 108.4, 71.8, 70.4, 68.7, 64.7, 58.9, 44.6. HRMS (ESI/TOF-Q): m/z [$\text{M} + \text{Na}$] $^+$ calcd for $\text{C}_{21}\text{H}_{25}\text{NO}_3\text{Na}$ 394.1630, found 394.1625.

Synthesis of Calix[n]carbazoles. A 1.0 g portion of compound **1** (2.7 mmol) and 0.29 g of $\text{FeCl}_3 \cdot 6\text{H}_2\text{O}$ (1 mmol) were first mixed in 1000 mL of DCM, and then 0.12 g of paraformaldehyde (4.0 mmol) was added to the solution. Eight hours later, 20 mL of water was added to the flask, the solvents were removed under vacuum, and the residue was dried under reduced pressure and then purified by flash chromatography on silica gel using MeOH/ CH_2Cl_2 (1:50, v/v) to give the desired cyclic products.

Data for Calix[3]carbazole. Yield: 206 mg, 20%. ^1H NMR (600 MHz, CDCl_3): δ 7.90 (s, 6H), 7.38 (d, $J = 8.3, 1.3$ Hz, 6H), 7.23 (d, $J = 8.3$ Hz, 6H), 4.99 (s, 6H), 4.29 (t, 6H), 4.27 (s, 6H), 3.64–3.62 (m, 6H), 3.57–3.55 (m, 6H), 3.52–3.48 (m, 18H), 3.35 (s, 9H). ^{13}C NMR (150 MHz, CDCl_3): δ 168.8, 139.7, 133.1, 127.2, 123.7, 120.5, 108.3, 72.0, 70.7, 70.7, 70.6, 68.9, 64.8, 59.2, 44.9, 41.6. HRMS (ESI/TOF-Q): m/z [$\text{M} + \text{H}$] $^+$ calcd for $\text{C}_{66}\text{H}_{76}\text{N}_3\text{O}_{15}$ 1150.5276, found 1150.5271.

Data for Calix[4]carbazole. Yield: 8 mg, 0.8%. ^1H NMR (600 MHz, CDCl_3): δ 7.70 (s, 8H), 7.33 (d, $J = 8.3$ Hz, 8H), 7.21 (d, $J = 8.3$ Hz, 8H), 4.97 (s, 8H), 4.28–4.26 (t, 8H), 4.21 (s, 8H), 3.63–3.59 (m, 8H), 3.55 (m, 8H), 3.52–3.45 (m, 24H), 3.34 (s, 12H). ^{13}C NMR (150 MHz, CDCl_3): δ 168.7, 139.6, 133.6, 127.3, 123.6, 120.8, 108.2, 72.0, 70.7, 70.7, 70.6, 68.9, 64.8, 59.2, 44.9, 42.0. HRMS (ESI/TOF-Q): m/z [$\text{M} + \text{Na}$] $^+$ calcd for $\text{C}_{88}\text{H}_{100}\text{N}_4\text{O}_{20}\text{Na}$ 1555.6829, found 1555.6820.

Data for Calix[5]carbazole. Yield: 67 mg, 6.5%. ^1H NMR (600 MHz, CDCl_3): δ 7.84 (s, 10H), 7.31 (dd, $J = 8.3, 1.4$ Hz, 10H), 7.20 (d, $J = 8.4$ Hz, 10H), 4.96 (s, 10H), 4.27–4.23 (m, 10H), 4.23 (s, 10H), 3.61–3.57 (m, 10H), 3.55–3.51 (m, 10H), 3.51–3.44 (m, 30H), 3.33 (s, 15H). ^{13}C NMR (150 MHz, CDCl_3): δ 168.5, 139.5, 133.3, 127.0, 123.4, 120.6, 108.4, 108.2, 71.9, 71.9, 70.5, 70.5, 68.8, 64.6, 58.9, 44.7, 41.9. HRMS (ESI/TOF-Q): m/z [$\text{M} + \text{Na}$] $^+$ calcd for $\text{C}_{110}\text{H}_{125}\text{N}_5\text{O}_{25}\text{Na}$ 1939.8595, found 1939.8578.

Data for Calix[6]carbazole. Yield: 51 mg, 5.0%. ^1H NMR (600 MHz, CDCl_3): δ 7.88 (s, 12H), 7.27 (dd, $J = 8.4, 1.4$ Hz, 12H), 7.19 (d, $J = 8.4$ Hz, 12H), 4.95 (s, 12H), 4.27–4.24 (m, 12H), 4.24 (s, 12H), 3.62–3.57 (m, 12H), 3.53 (m, 12H), 3.50–3.44 (m, 36H), 3.32 (s, 18H). ^{13}C NMR (150 MHz, CDCl_3): δ 168.7, 139.5, 133.5, 127.2, 123.4, 120.8, 108.4, 71.9, 70.6, 70.58, 70.6, 68.9, 64.7, 59.1, 44.8, 41.9. HRMS (ESI/TOF-Q): m/z [$\text{M} + \text{Na}$] $^+$ calcd for $\text{C}_{132}\text{H}_{150}\text{N}_6\text{O}_{30}\text{Na}$ 2323.0328, found 2323.0320.

■ ASSOCIATED CONTENT

Supporting Information

The Supporting Information is available free of charge on the ACS Publications website at DOI: 10.1021/acs.joc.6b00252.

NMR and HRMS spectra of the synthesized compounds, VT NMR and ^1H NMR spectra of **2** at different concentrations, UV-vis, fluorescence, and IR spectra, 2D NMR spectra of **2** in the absence and presence of guests, Job plot and HRMS spectrum of **2**-TEA complexation, 1D ^1H NMR titration spectra, determination of association constants, and molecular models (PDF)

■ AUTHOR INFORMATION

Corresponding Author

*E-mail: yangpeng@syphu.edu.cn, pengyangcn05@hotmail.com.

Author Contributions

† Y.J. and X.Z. contributed equally to this work.

Notes

The authors declare no competing financial interest.

■ ACKNOWLEDGMENTS

We acknowledge support from the National Natural Science Foundation of China (Grant 21102095), Liaoning Provincial Natural Science Foundation (Grant 2015020752), and programs for the innovative research team of the Ministry of Education and for the Liaoning innovative research team in university. The measurements of VT NMR spectra were performed at the Center for Physicochemical Analysis and Measurement at the Institute of Chemistry of the Chinese Academy of Sciences (ICCAS). Help from Dr. Jun-feng Xiang is acknowledged.

■ REFERENCES

- (1) (a) Lehn, J.-M. *Science* **1993**, *260*, 1762. (b) Thordarson, P.; Bjirsterveld, E. J.; Rowan, A. E.; Nolte, R. J. *Nature* **2003**, *424*, 915. (c) Le Poul, N.; Le Mest, Y.; Jabin, I.; Reinaud, O. *Acc. Chem. Res.* **2015**, *48*, 2097.
- (2) (a) Sussman, J. L.; Harel, M.; Frolow, F.; Oefner, C.; Goldman, A.; Toker, L.; Silman, I. *Science* **1991**, *253*, 872. (b) Ma, J. C.; Dougherty, D. A. *Chem. Rev.* **1997**, *97*, 1303.
- (3) (a) Ghasemabadi, G. P.; Yao, T.; Bodwell, G. J. *Chem. Soc. Rev.* **2015**, *44*, 6494. (b) Gutsche, C. D. *Calixarenes*; The Royal Society of Chemistry: Cambridge, U.K., 1989. (c) Corbellini, F.; Mulder, A.; Sartori, A.; Ludden, M. J. W.; Casnati, A.; Ungaro, R.; Huskens, J. M.; Crego-Calama, M.; Reinhoudt, D. N. *J. Am. Chem. Soc.* **2004**, *126*, 17050. (d) Gibb, C. L. D.; Stevens, E. D.; Gibb, B. C. *J. Am. Chem. Soc.* **2001**, *123*, 5849. (e) Zimmermann, H.; Tolstoy, P.; Limbach, H. H.; Poupkov, R.; Luz, Z. *J. Phys. Chem. B* **2004**, *108*, 18772. (f) Ogoshi, T.; Kanai, S.; Fujinami, S.; Yamagishi, T.; Nakamoto, Y. *J. Am. Chem. Soc.* **2008**, *130*, 5022. (g) Custelcean, R.; Delmau, L. H.; Moyer, B. A.; Sessler, J. L.; Cho, W. S.; Gross, D.; Bates, G. W.; Brooks, S. J.; Light, M. E.; Gale, P. A. *Angew. Chem., Int. Ed.* **2005**, *44*, 2537. (h) Black, D. St.C.; Craig, B. D. C.; Kumar, N. *Tetrahedron Lett.* **1995**, *36*, 8075.

(i) Georghiou, P. E.; Ashram, M.; Li, Z.; Chaulk, S. G. *J. Org. Chem.* **1995**, *60*, 7284.

(4) (a) Rebek, J., Jr. *Acc. Chem. Res.* **2009**, *42*, 1660. (b) Yoshizawa, M.; Klosterman, J. K.; Fujita, M. *Angew. Chem., Int. Ed.* **2009**, *48*, 3418. (c) Brown, C. J.; Toste, F. D.; Bergman, R. G.; Raymond, K. N. *Chem. Rev.* **2015**, *115*, 3012. (d) Garel, L.; Lozach, B.; Dutasta, J. P.; Collet, A. *J. Am. Chem. Soc.* **1993**, *115*, 11652.

(5) (a) Li, G.; Zhou, X.; Yang, P.; Jian, Y.; Deng, T.; Shen, H.; Bao, Y. *Tetrahedron Lett.* **2014**, *55*, 7054. (b) Yang, P.; DeCian, A.; Teulade-Fichou, M. P.; Mergny, J. L.; Monchaud, D. *Angew. Chem., Int. Ed.* **2009**, *48*, 2188. (c) Monchaud, D.; Yang, P.; Lacroix, L.; Teulade-Fichou, M. P.; Mergny, J. L. *Angew. Chem., Int. Ed.* **2008**, *47*, 4858.

(6) Strohrriegel, P.; Grazulevicius, J. V. In *Handbook of Organic Conductive Molecules and Polymers*; Nalwa, H. S., Ed.; Wiley: New York, 1997; Vol. 1, pp 553–620.

(7) Gale, P. A. *Chem. Commun.* **2008**, 4525.

(8) Schmidt, A. W.; Reddy, K. R.; Knölker, H.-J. *Chem. Rev.* **2012**, *112*, 3193.

(9) (a) Piątek, P.; Lynch, V. M.; Sessler, J. L. *J. Am. Chem. Soc.* **2004**, *126*, 16073. (b) Kondratowicz, M.; Myśliwiec, D.; Lis, T.; Stępień, M. *Chem. - Eur. J.* **2014**, *20*, 14981.

(10) Lowen, S. V.; Buschek, J.; Mastantuono, R.; Holden, D. A.; Kovacs, G. J.; Loutfy, R. O. *Macromolecules* **1990**, *23*, 3242.

(11) Roelens, S.; Torriti, R. *J. Am. Chem. Soc.* **1998**, *120*, 12443.

(12) Ohkita, H.; Ito, S.; Yamamoto, M.; Tohda, Y.; Tani, K. *J. Phys. Chem. A* **2002**, *106*, 2140.

(13) (a) Hu, J.; Barbour, L. J.; Gokel, G. W. *J. Am. Chem. Soc.* **2002**, *124*, 10940. (b) Okada, A.; Miura, T.; Takeuchi, H. *Biochemistry* **2001**, *40*, 6053.

(14) (a) Mugridge, J. S.; Zahl, A.; van Eldik, R.; Bergman, R. G.; Raymond, K. N. *J. Am. Chem. Soc.* **2013**, *135*, 4299. (b) Gangopadhyay, M.; Mandal, A. K.; Maity, A.; Ravindranathan, S.; Rajamohanan, P. R.; Das, A. *J. Org. Chem.* **2016**, *81*, 512. (c) Hu, J. J.; Cheng, Y. Y.; Ma, Y. R.; Wu, Q. L.; Xu, T. W. *J. Phys. Chem. B* **2009**, *113*, 64. (d) Chai, M. H.; Niu, Y. H.; Youngs, W. J.; Rinaldi, P. L. *J. Am. Chem. Soc.* **2001**, *123*, 4670.

(15) Spartan'14 for Windows (version 1.1.4, Wave Function, Inc., Irvine, CA, 2014) was used to minimize the geometry of complexation at the PM₃ level. The non-recognition-involved moieties were omitted for the sake of both clarity and calculation expense. See the details in the [Supporting Information](#).

(16) Connors, K. A. *Binding Constants*; Wiley: New York, 1987.

(17) (a) Arduini, A.; Giorgi, G.; Pochini, A.; Secchi, A.; Ugozzoli, F. *J. Org. Chem.* **2001**, *66*, 8302. (b) Kubik, S. *J. Am. Chem. Soc.* **1999**, *121*, 5846.

(18) Jeong, K.-S.; Hahn, K.-M.; Cho, Y. L. *Tetrahedron Lett.* **1998**, *39*, 3779.

(19) Tian, Y.-P.; Zhang, X.-J.; Wu, J.-Y.; Fun, H.-K.; Jiang, M.-H.; Xu, Z.-Q.; Usman, A.; Chantrapromma, S.; Thompson, L. K. *New J. Chem.* **2002**, *26*, 1468.